Electronic Supplementary Information

Self-healing polyurethane with high strength and toughness based on dynamic chemical strategy

Fuhao Dong,[†a] Xinxin Yang,[†b] Lizhen Guo,[b] Yuqi Wang,[a] Hiba Shaghaleh,[a] Zhen Huang,[a] Xu Xu,[*a] Shifa Wang [*a] and He Liu [*b]

a. College of Chemical Engineering, Nanjing Forestry University, Co-Innovation Center of Efficient Processing and Utilization of Forest Resources, Jiangsu Provincial Key Lab for the Chemistry and Utilization of Agro-forest Biomass, Nanjing 210037, Jiangsu Province, China.

b. Institute of Chemical Industry of Forestry Products, Chinese Academy of Forestry, Key Laboratory of Biomass Energy and Material, National Engineering Laboratory for Biomass Chemical Utilization, Key and Open Laboratory of Forest Chemical Engineering, State Forestry Administration, Nanjing 210042, Jiangsu Province, China.

[†]These authors contributed equally to this work.

*Corresponding authors: Email: xuxu200121@hotmail.com (X. X.), wangshifa65@163.com (S. W.), liuhe.caf@gmail.com (H. L.)

Results and Discussion

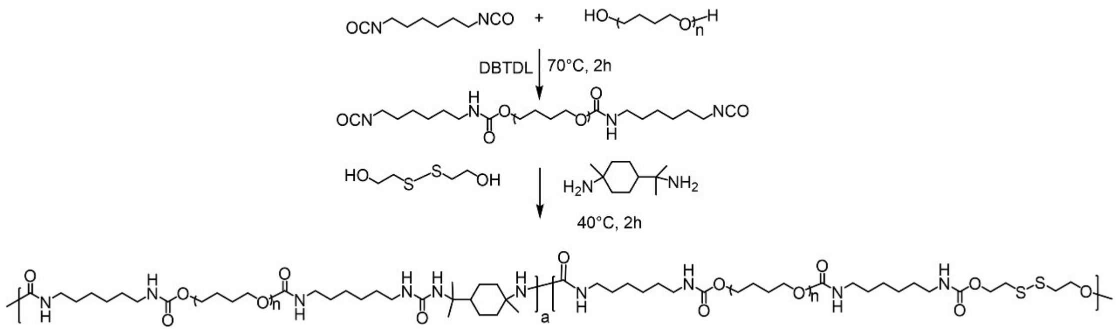

Figure S1. Synthetic routes of MD-PU-SS.

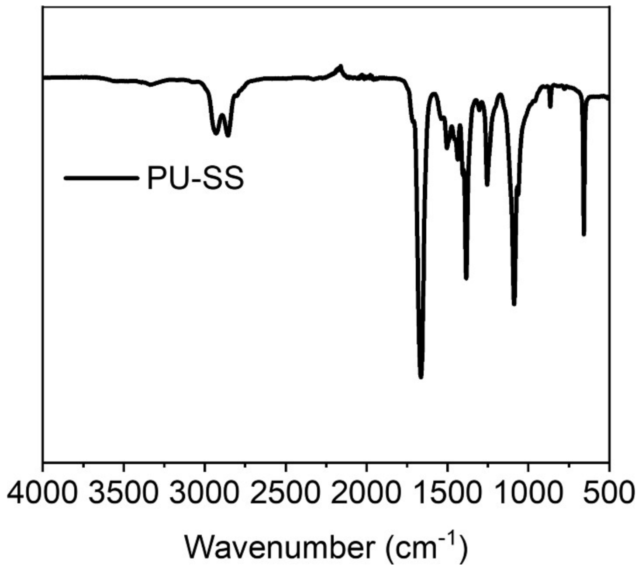

Figure S2. FTIR spectra of the PU-SS.

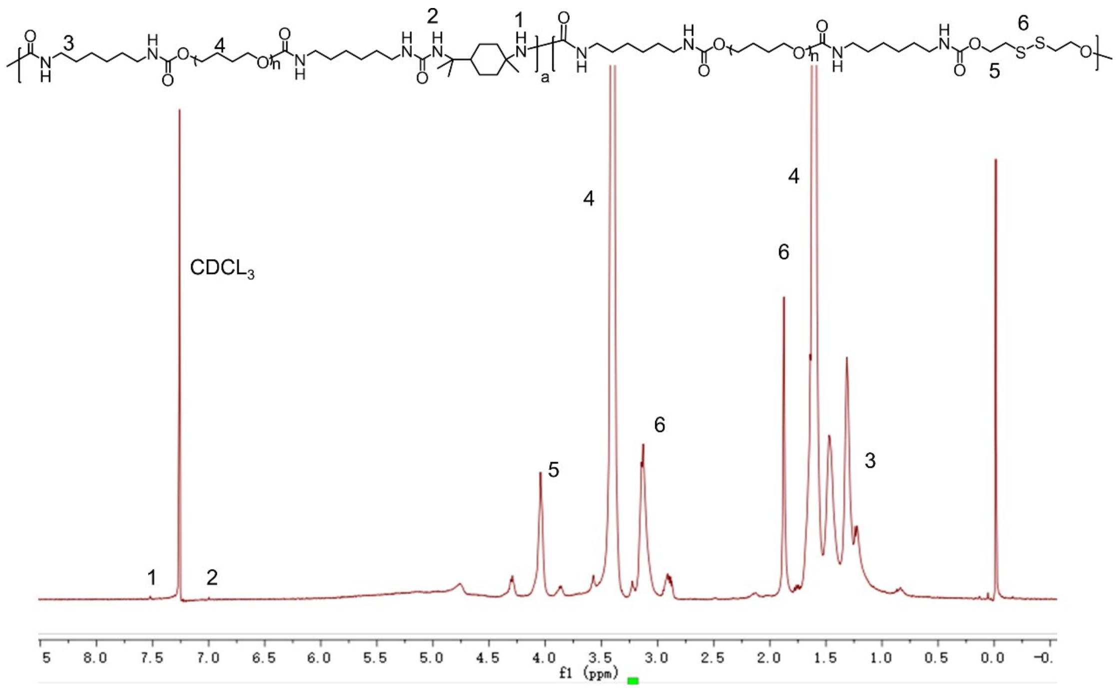

Figure S3. ^{1}H NMR of MD-PU-SS (400 MHz, $CDCl_3$, 25 °C).

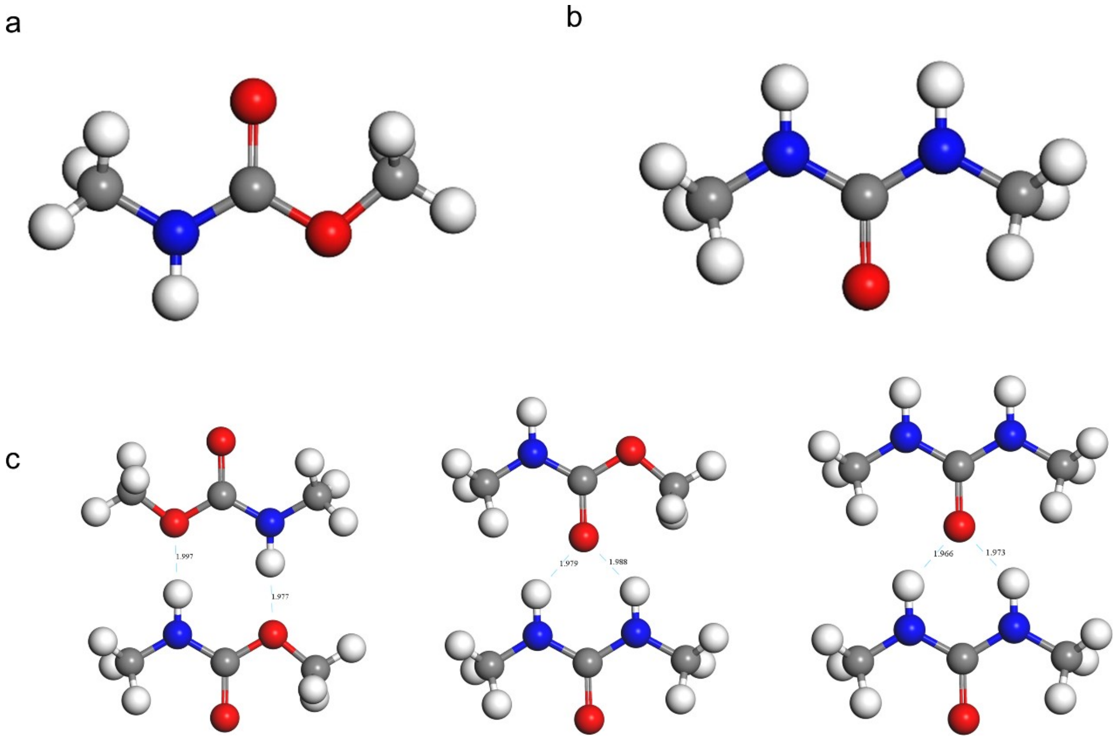

Figure S4. Optimized molecular structures for simulation. a) Monomer A, b) Monomer B. c) Bonding energy of three types of individual H-bond, including urea–carbamate interaction, carbamate–carbamate interaction and urea–urea interaction.

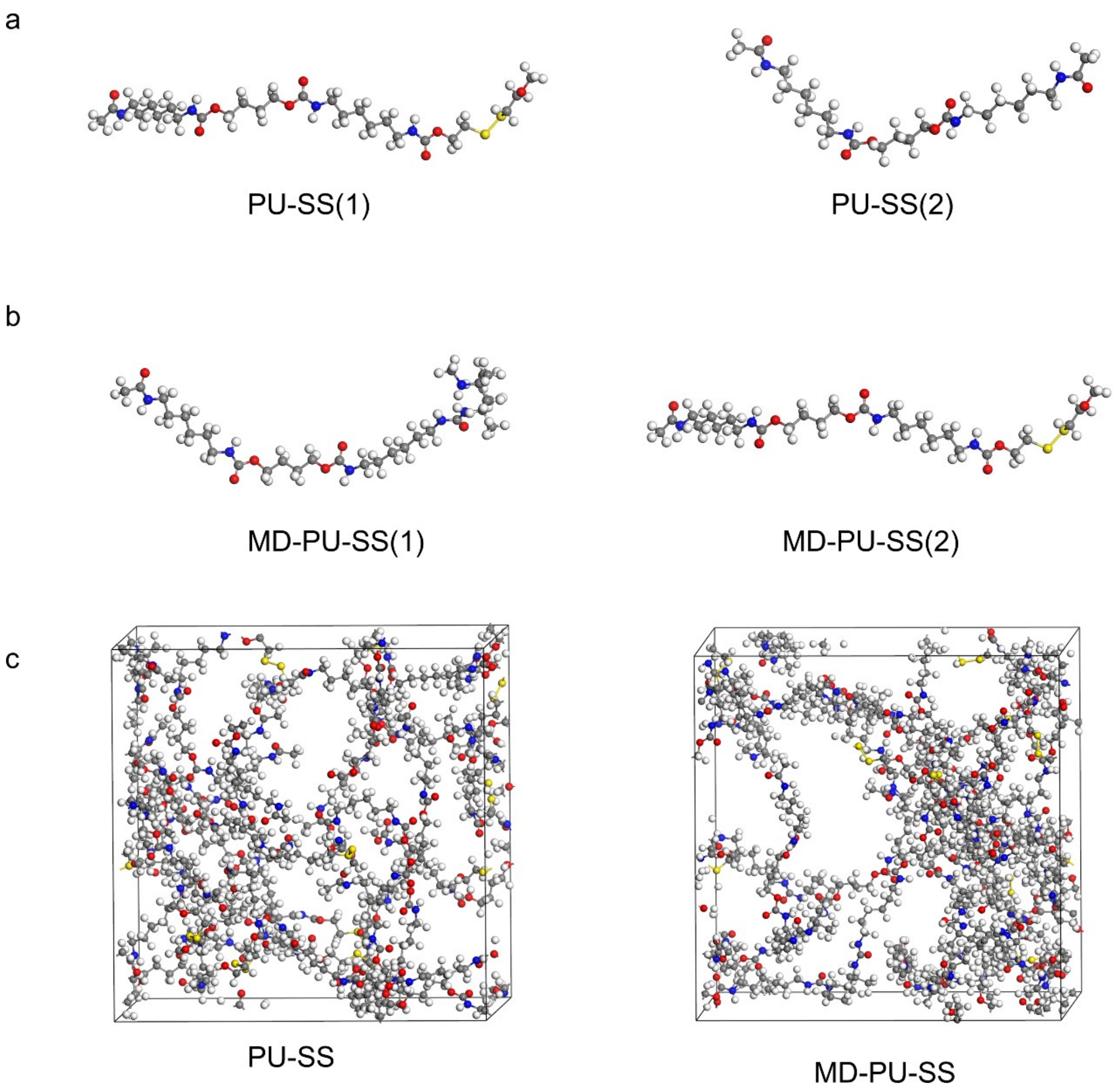

Figure S5. Quantum chemical simulation of hard domains. a, b) Optimized hard segments for simulations. c)The initial configuration of two elastomers.

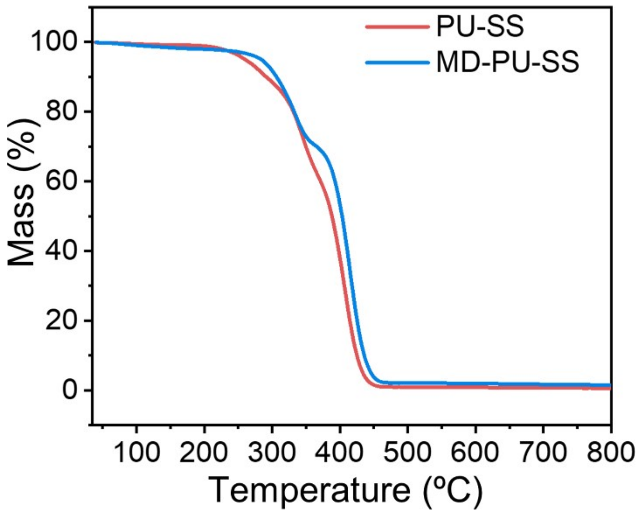

Figure S6. TGA curves of the PU-SS and MD-PU-SS under N_2 atmosphere.

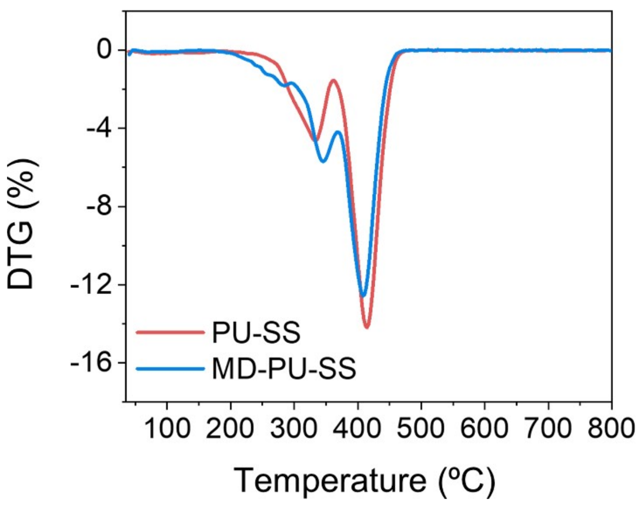

Figure S7. DTG curves of PU-SS and MD-PU-SS under N_2 atmosphere.

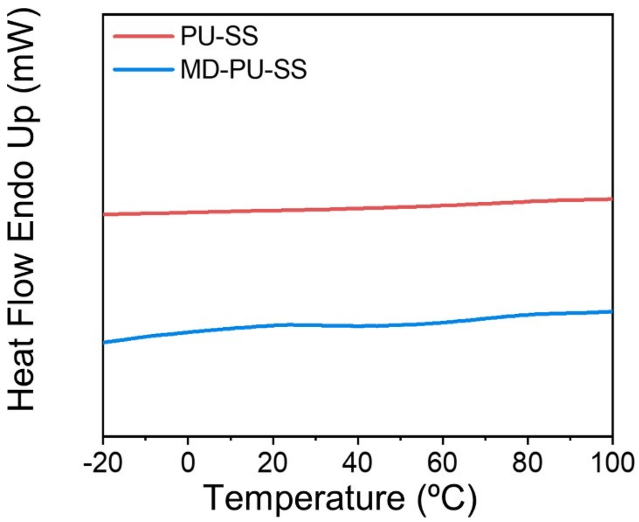

Figure S8. DSC of PU-SS and MD-PU-SS.

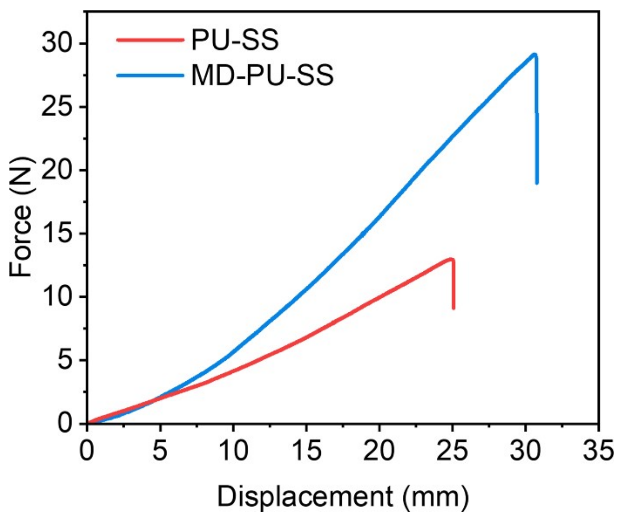

Figure S9. Puncture testing result of PU-SS and MD-PU-SS.

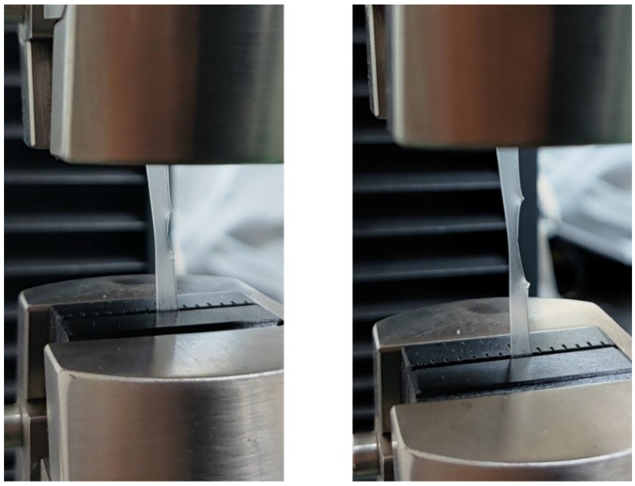

Figure S10. Photographs of the notched MD-PU-SS sample that is elongated to different strains.

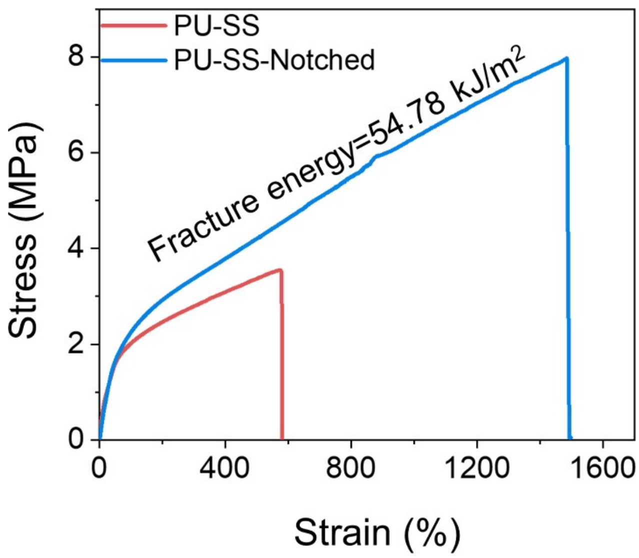

Figure S11. Stress-strain curves of the unnotched and notched PU-SS, which are used for the calculation of the fracture energy.

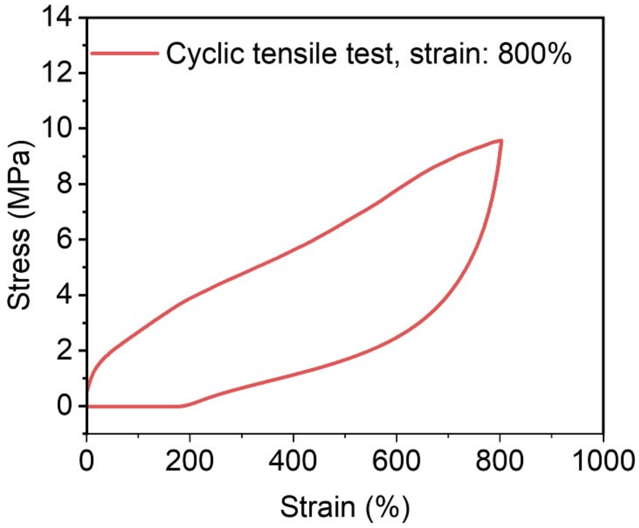

Figure S12. Cyclic tensile test of MD-PU-SS at 800% strain.

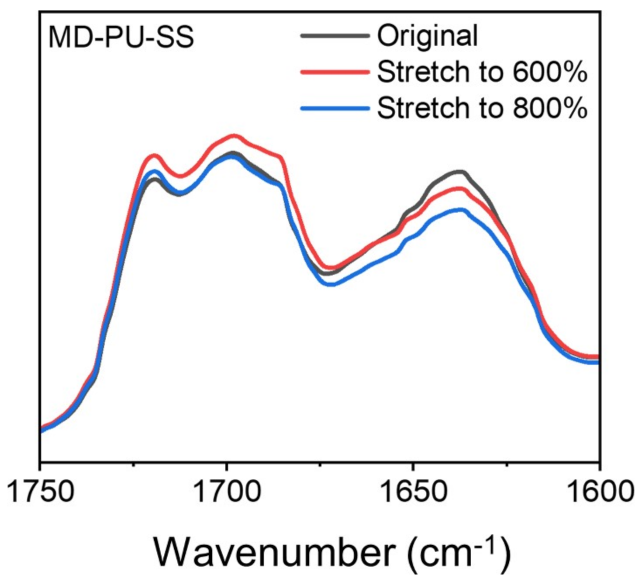

Figure S13. FTIR spectra of the MD-PU-SS in the C=O stretching region, measured at different strains.

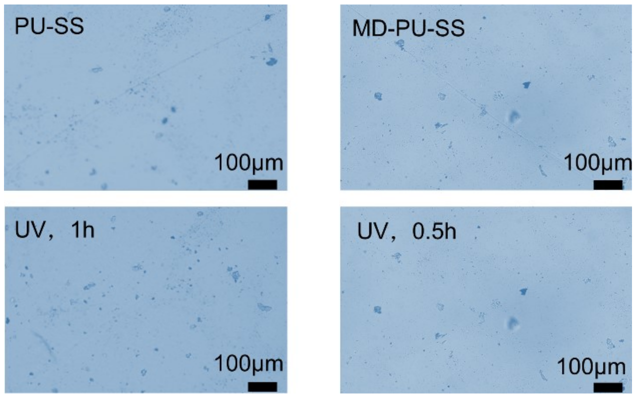

Figure S14. Self-healing of PU-SS and MD-PU-SS under UV irradiation.

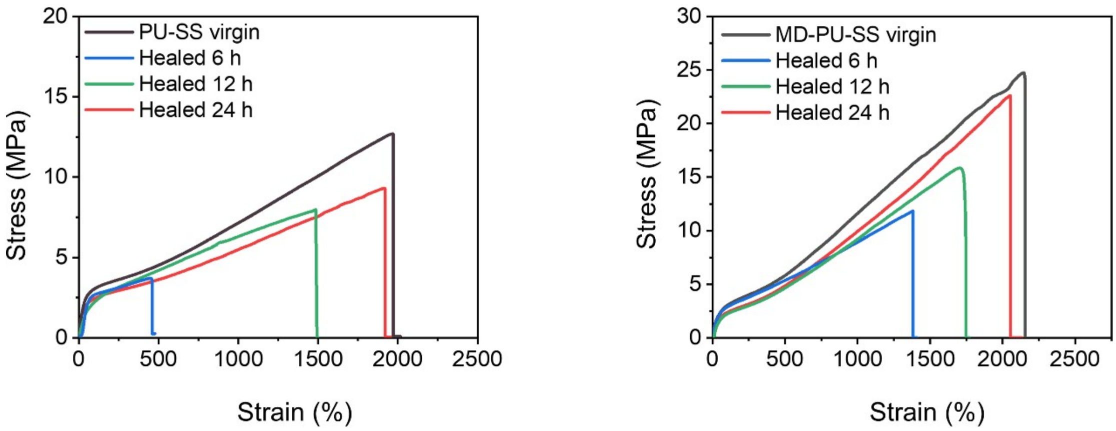

Figure S15. Stress–strain curves of virgin and scratched PU-SS and MD-PU-SS specimens at different self-healing time under 60 °C.

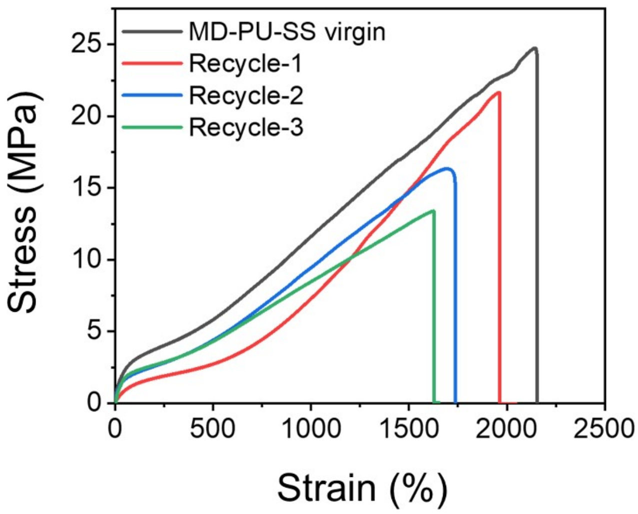

Figure S16. Stress−strain curves after hot pressing.

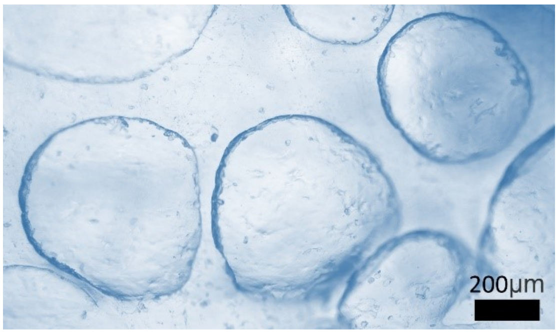

Figure S17. Optical microscopy images of recycled polyurethane elastomer.

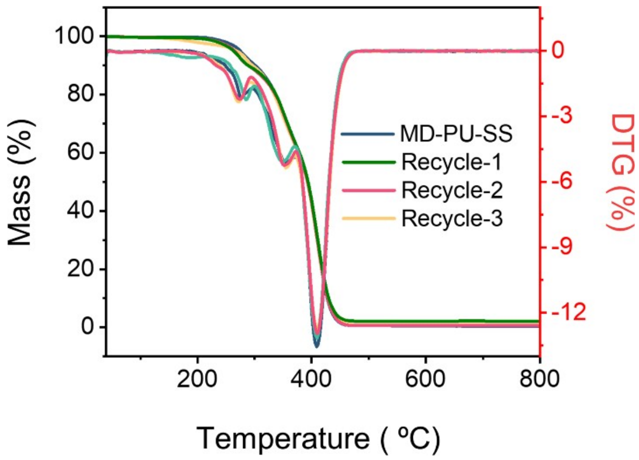

Figure S18. TGA and DTG curves after hot pressing.

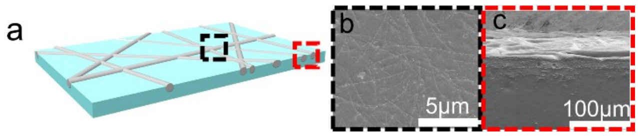

Figure S19. a) Illustration of an enlarged view of the MD-PU-SS/AgNW conductor. b, c) Surface and cross-sectional SEM images of the MD-PU-SS/AgNW conductor.

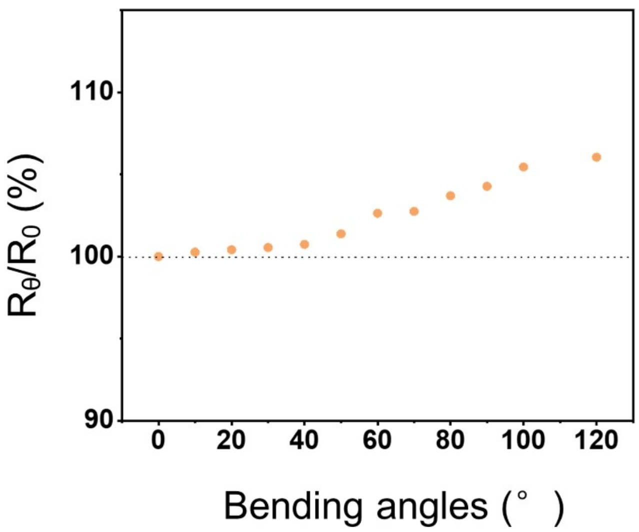

Figure S20. The electric resistance ratio of the as-fabricated conductor bend under diverse bending angel.

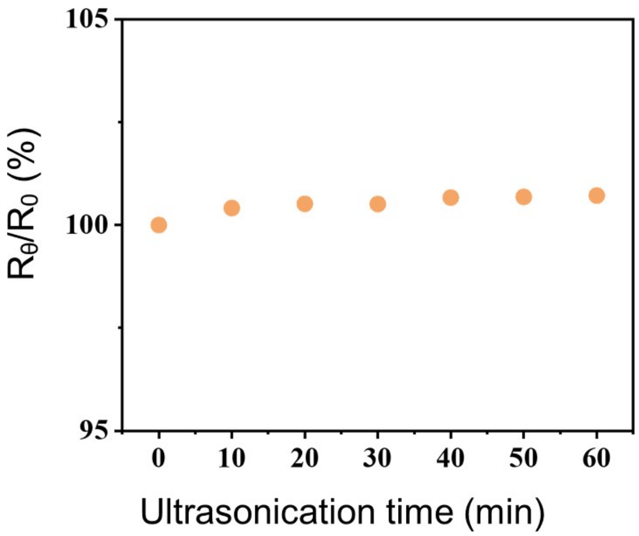

Figure S21. Resistance changes of MD-PU-SS/AgNW conductor after ultrasonic treatment

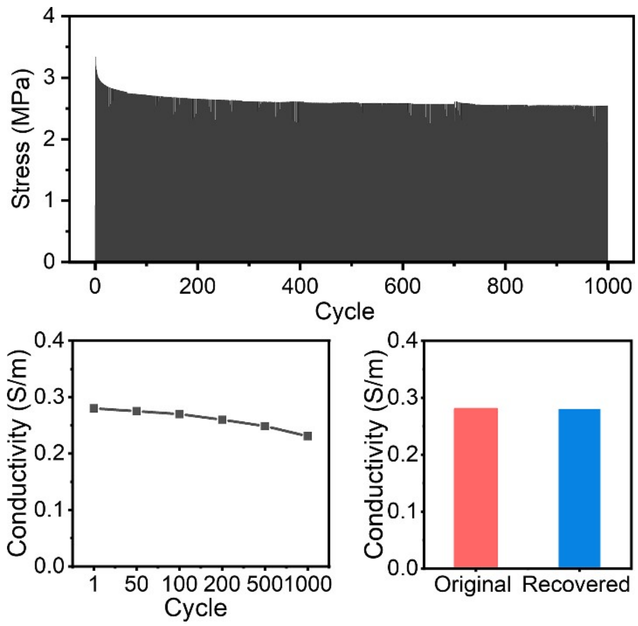

Figure S22. a) Cyclic tensile test of MD-PU-SS/AgNW conductor at 100% strain for 1000 times b) The conductivity of MD-PU-SS/AgNW conductor via treating with certain number of cyclic tensile test at 100% strain c) The conductivity of the recovering MD-PU-SS/AgNW conductor after 1000 times of cycling.

Table S1. Formulas of the PU-SS and MD-PU-SS.

Sample code	PTMEG (g)	HDI (g)	HEDS (g)	MD (g)	Molar Ratio of (PTMEG:HDI:HEDS:MD)
PU-SS	20	10.43	6.48	----	1 : 3.1 : 2.1 : 0
MD-PU-SS	20	12.11	6.48	1.70	1 : 3.6 : 2.1 : 0.5

Table S2. GPC results of PU-SS and MD-PU-SS.

Sample code	Mn (g/mol)	Mw (g/mol)	PDI
PU-SS	50700	76500	1.50
MD-PU-SS	43100	85600	1.98

Table S3. Summary of the mechanical properties of PU-SS and MD-PU-SS.

Samples code	Tensile stress (MPa)	Elongation-at-break (%)	Toughness (MJ m^{-3})	True stress at break (MPa)	True strain at break (ln mm mm^{-1})
PU-SS	12.7±2.1	1968.1±100.6	143.3±11.2	263.8±45.6	3.0±0.08
MD-PU-SS	24.8±1.8	2144.7±103.4	274.6±22.8	557.0±32.7	3.1±0.06

Table S4. Comparison of stress, strain, self-healing efficiency, self-healing strain, self-healing stress, and healing temperature of various self-healing polymers

Sample code	Healing temperature (°C)	Stress (MPa)	Strain (%)	Self-healing stress (MPa)	Self-healing strain (%)	Self-healing ratio (%)
This work	40	24.8	2143	23.3	2047	94
Poly(urea-urethane)-Exchangeable urea bond	60	3.8	690	2.5	590	66
PU-Aliphatic disulfide	25	19.4	1410	17	1300	88
PU-Boronic Ester Bond	25	4.15	947	3.7	970	89
Rubber-Disulfude	90	1.3	270	1.3	370	1
PDMS-Fe^{3+} H-bonds	70	2.8	1475	2.7	1370	96
PU-Disulfid bond	55	3.39	400	3.1	340	91
PU-Aromatic disulfide	25	6.8	910	5.9	907	87
PU-Aromatic disulfide	25	9.4	630	9.1	610	97
Rubber-Zn^{+} H-bonds	90	21	560	16	550	76
PU-Aliphatic disulfide	100	13	810	12.7	815	98
TBP-Aliphatic disulfide	25	0.24	105	0.21	100	88
PU-Aliphatic disulfide	80	22	830	17	800	77
Rubber-Zinc dimethacrylate	60	0.62	340	0.61	290	98